European Journal of Pharmaceutics and Biopharmaceutics 80 (2012) 368–378

Contents lists available at SciVerse ScienceDirect

European Journal of Pharmaceutics and Biopharmaceutics

journal homepage: www.elsevier.com/locate/ejpb

Research paper

A novel small Odorranalectin-bearing cubosomes: Preparation, brain delivery and pharmacodynamic study on amyloid-β_{25-35}-treated rats following intranasal administration

Hongbing Wu [a,c,1], Jianxu Li [b,1], Qizhi Zhang [a], Xiluan Yan [a], Liangran Guo [a], Xiaoling Gao [d], Mingfeng Qiu [c], Xinguo Jiang [a,*], Ren Lai [b], Hongzhuan Chen [d]

[a] School of Pharmacy, Fudan University, Shanghai, China
[b] Kunming Institute of Zoology, Chinese Academy of Sciences, Kunming, China
[c] School of Pharmacy, Shanghai Jiaotong University, Shanghai, China
[d] Department of Pharmacology, Shanghai Jiaotong University School of Medicine, Shanghai, China

ARTICLE INFO

Article history:
Received 13 May 2011
Accepted in revised form 14 October 2011
Available online 28 October 2011

Keywords:
Odorranalectin
Cubosomes
Intranasal administration
Gly14-Humanin
Brain delivery
Alzheimer's disease

ABSTRACT

Because of the immunogenicity and toxicity *in vivo* of large molecules such as lectins, the application of these molecules is remarkably restricted in drug delivery systems. In this study, to improve the brain drug delivery and reduce the immunogenicity of traditional lectin modified delivery system, Odorranalectin (OL, 1700 Da), a novel non-immunogenic small peptide, was selected to establish an OL-modified cubosomes (Cubs) system. The streptavidin (SA)-conjugated Cubs were prepared by incorporating maleimide–PEG–oleate and taking advantage of its thiol group binding reactivity to conjugate with 2-iminothiolane thiolated SA; mono-biotinylated OL was then coupled with the SA-modified Cubs. The OL-decorated Cubs (OL-Cubs) devised *via* a non-covalent SA-biotin "bridge" made it easy to conjugate OL and determine the number of ligands on the surface of the Cubs using sensitive chemiluminescent detection. Retention of the bio-recognitive activity of OL after covalent coupling was verified by hemagglutination testing. Nose-to-brain delivery characteristic of OL-Cubs was investigated by *in vivo* fluorescent biodistribution using coumarin-6 as a marker. The relative uptake of coumarin carried by OL-Cubs was 1.66- to 3.46-fold in brain tissues compared to that incorporated in the Cubs. Besides, Gly14-Humanin (S14G-HN) as a model peptide drug was loaded into cubosomes and evaluated for its pharmacodynamics on Alzheimer's disease (AD) rats following intranasal administration by Morris water maze test and acetylcholinesterase activity determination. The results suggested that OL functionalization enhanced the therapeutic effects of S14G-HN-loaded cubosomes on AD. Thus, OL-Cubs might offer a novel effective and noninvasive system for brain drug delivery, especially for peptides and proteins.

1. Introduction

Being influenced by the frantic rhythm of life, population aging, environmental factor, traffic accidents and so on, brain diseases are becoming more and more serious threaten of human health with yearly progressive increase. Fortunately, the development of neuroscience has facilitated the discoveries of proteins [1] and peptides [2] with considerable potential in the treatment of central nervous system (CNS) diseases such as Alzheimer's disease (AD) and Parkinson disease. Thus, there is an increasing need of novel brain drug carriers for macromolecular drugs in the treatment of CNS disorders.

Direct nose-to-brain delivery of therapeutics, bypassing the blood–brain barrier (BBB), has provided a noninvasive and effective route for the treatment of CNS disorders. Numerous successful studies focusing on the nasal pathway for CNS drug delivery have been reported [3,4]. However, the uptake of drugs in the brain is reported to be low, especially nasally applied macromolecular drugs such as peptides, proteins and DNA, which are poorly absorbed and highly susceptible to the harmful environment of the nasal cavity. Incorporation of these drugs into polymeric nanoparticles, polymersomes [5] or liposomes might be a promising approach, since colloidal carrier systems have been shown to protect compounds from the degrading milieu in the nasal cavity and facilitate their transport across the mucosal barriers [6]. However, these nanocarriers still bear the problems of low drug encapsulation efficiency and payload, residual solvent and non-bioadhesive [7]. In recent years, by virtue of a variegated range of encapsulation, high drug payloads and stabilization of peptides

* Corresponding author. School of Pharmacy, Fudan University, Shanghai 201203, China. Tel.: +86 21 51980067; fax: +86 21 51980069.
E-mail address: xgjiang@shmu.edu.cn (X. Jiang).
[1] These authors contributed equally to this work.

0939-6411/$ - see front matter © 2011 Elsevier B.V. All rights reserved.
doi:10.1016/j.ejpb.2011.10.012

[8,9] or proteins [10–13], cubic phase structures self-assembled using amphiphilic materials when present in an aqueous environment have become the focus of drug delivery systems. Cubosomes (Cubs) are discrete, submicron, nanostructured particles of bicontinuous cubic liquid crystalline phase, which are able to incorporate large amounts of drugs of varying physicochemical properties and can be localized in body cavities, on the skin or on different mucosal surfaces [14]. Cubs consisting of amphiphilic lipoid materials, such as glyceryl monooleate (GMO), have a stiff, bioadhesive and gel-like appearance and are degradable and innoxious in the human body [15]. In spite of academic [16,17] and commercial interests, there are few reports of studies on nasally administered Cubs for drug brain delivery. Nevertheless, as with plain-nanovehicles in nasal application, on the one hand, mucociliary clearance limits the time available for drug absorption, and on the other hand, selective transport (for drug targeting to the brain) following mucosal absorption is difficult to realize. Therefore, modified nanovehicles with both mucoadhesive properties and enhanced specific delivery to the brain might eliminate the obstacles related to drug brain delivery *via* the nasal route and offer an ideal alternative.

One approach to improve the mucoadhesive ability of nanoparticles is surface modification with bio-recognitive ligands such as lectins, of which the potential to act as drug delivery adjuvants is increasing [18–21]. In spite of the interesting biological potential of lectin for drug targeting and delivery, a potential disadvantage of natural lectins is the large size of these molecules, which results in immunogenicity and toxicity. Smaller peptides that can mimic the function of lectins are promising candidates for drug targeting. Odorranalectin (OL) from the skin secretions of the amphibian *Odorrana grahami*, specifically binds to L-fucose [22], which was shown to have greater expression on olfactory mucosa than on respiratory mucosa [23,24], is the smallest lectin (MW 1.7 kDa) [25] and was selected as a model ligand to enhance the binding of cubosomes to nasal mucosa and improve drug brain uptake.

S14G-HN, a derivative of Humanin (HN) with substitution of glycine for serine 14, shown about 1000-fold neuroprotective activity than HN [26], is a novel 24-amino acid peptide and effective at low concentrations against memory impairment caused by AD-related insults [27,28]. As a very promising anti-AD drug, S14G-HN has a high specificity and low doses merits. However, the peptide is hard to cross the BBB and easy to be metabolized by deactivation under internal circumstances, intravenous administration is difficult to achieve an ideal efficacy, and it often needs intraventricular injection [29]. So far, only Colivelin [30] (a hybrid peptide of HN and neurotrophic factor) and the other HN derivatives [31] reported were intranasally administered against memory impairment of AD models. And there are little reports about S14G-HN preparations for intranasal administration in rats. The lack of effective carriers and a convenient administration are the main problems or common failing of these macromolecular drugs brain delivery. Therefore, S14G-HN was selected as a model drug in this study.

In brief, the present study attempted to develop a protocol for the surface engineering of poly (ethylene glycol) (PEG)-ylated cubosomes with OL (OL-Cubs) and to evaluate its brain delivery following intranasal administration. To do this, maleimide–PEG–oleate was synthesized and blended with 1-Monoolein and Pluronic F127 to prepare the cubosomes by dilution–sonication [32]. The resulting cubosomes were then functionalized with thiolated streptavidin (SA) by taking advantage of the thiol group coupling activity of maleimide. The mono-biotinylated OL (homing molecule) was then coupled to the cubosomes by a "bridge" of SA-biotin and a PEG compound linker (Fig. 1). Coumarin-6, a lipophilic fluorescent probe with high sensitivity, was incorporated into cubosomes to investigate the brain distribution of OL-Cubs *in vivo*. In

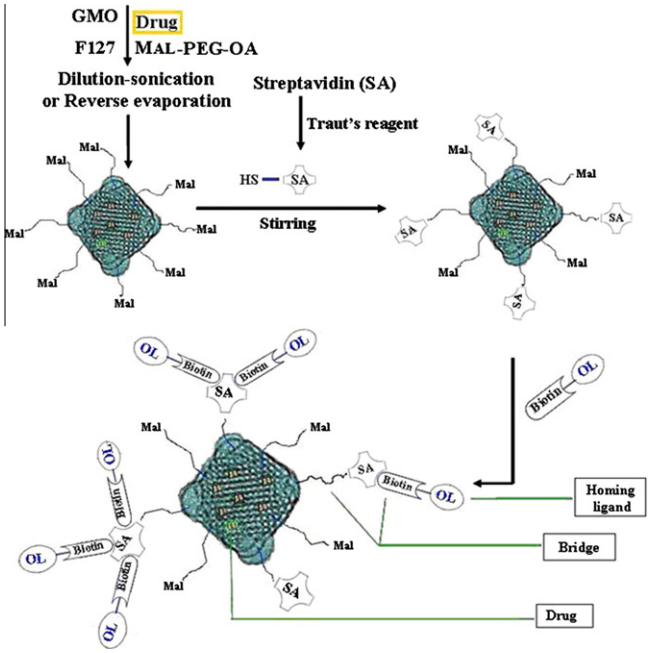

Fig. 1. Schematic illustration of preparing drug-loaded cubosome decorated by OL. The "sponge" structure self-assembled is composed of a common surfactant GMO and polymeric stabilizer Pluronic F127, with lipophilic (dilution–sonication method) or hydrophilic (reverse evaporation method) drugs encapsulation. (For interpretation of the references to color in this figure legend, the reader is referred to the web version of this article.)

the pharmacodynamic study, neuroprotective effect of the S14G-HN-loaded OL-Cubs was tested in $A\beta_{25-35}$-treated rats following intranasal administration.

2. Materials and methods

2.1. Materials and animals

1-Monoolein, denoted as RYLO™ MG pharma 19 glycerol monooleate (GMO), was a generous gift from Danisco (China) Co., Ltd. (Shanghai). PEO_{98}–PPO_{67}–PEO_{98} triblock copolymer (F127) was obtained from BASF Svenska AB (Helsingborg, Sweden). Maleimide poly (ethylene glycol) (MAL–PEG, MW 3500 Da, purity more than 90%) was supplied by Beijing JenKem Technology Co., Ltd. Oleoyl chloride, 6-coumarin, 2-iminothiolane hydrochloride (2-IT) and streptavidin (SA) were all purchased from Sigma–Aldrich (Shanghai) Trading Co., Ltd. Triethylamine (TEA) and dichloromethane were freshly dried according to conventional methods. Streptavidin-modified polystyrene beads (0.56 μm) were purchased from Bangs Laboratories; 5,5-dithiobis (2-nitrobenzoic acid) (Ellman's reagent) was from Acros (Belgium). The biotinylated Odorranalectin (biotin-YASPKCFRYPNGVLACT, biotin-OL, purity by HPLC >95%) and S14G-Humanin (purity by HPLC >95%) were both customized by GL Biochem (Shanghai) Ltd. Double-distilled water was purified by a Millipore Simplicity System (Millipore, Bedford, MA, USA). All other chemicals used were of analytical grade and without further purification.

Sprague-Dawley rats (180–220 g, ♀, License number: SCXK (Hu) 2008-0016) were obtained from the Experimental Animal Center of Fudan University and maintained at 22 ± 2 °C on a 12 h light-dark cycle with *ad libitum* access to food and water. Toads (30–40 g, ♂♀), also purchased from the Experimental Animal Center of Fudan University, were kept in moist conditions with free access to food and water. The animals used for the experiments were treated according to protocols evaluated and approved by the ethical committee

of Fudan University. All efforts were made to minimize animals suffering.

2.2. Synthesis and characterization of maleimide–PEG–oleate (MAL–PEG–OA)

MAL–PEG–OA was synthesized by reacting oleoyl chlorides with one hydroxyl-terminated MAL–PEG according to previously published reports [33,34]. The structure of MAL–PEG–OA was studied by ^{1}H NMR spectroscopy at 400 MHz using D-chloroform as a solvent. The relative molecular weight of MAL–PEG–OA was determined by a gel permeation chromatography (GPC) system (Waters 1515 Isocratic HPLC pump, 2414 refractive index detector and a set of Waters Styragel columns). Details of the synthesis and characterization of MAL–PEG–OA were given in Appendix A.

2.3. Preparation of functionalized Cubs

2.3.1. Preparation of PEGylated Cubs

PEGylated Cubs were prepared using a blend of MAL–PEG–OA, GMO and F127 and the dilution–sonication technique adopted by Spicer [32]. Briefly, 1 mL ethanol solution was used to dissolve the GMO (90 mg/mL), and MAL–PEG–OA (5 mg/mL) was injected into 2 mL F127 (in 10 mmol/L phosphate buffer solution (PBS), pH 7.4) at a weight ratio of GMO/F127/MAL–PEG–OA/H_2O = 4.5/0.25/0.25/95, with magnetic stirring. Half an hour later, ethanol was evaporated under reduced pressure at 40 °C. Then, in ice-water bath conditions, the coarse dispersions were processed by sonication (200 w, 40 s) using a probe sonicator (Scientz Biotechnology Co., Ltd., China). 6-coumarin-loaded cubosomes were prepared by the same procedure except that 0.1% (w/v) of 6-coumarin was added to the ethanol solution before pouring into the aqueous phase and the obtained cubosomes were subjected to a 1.5 × 20 cm sepharose CL-4B column and eluted with 10 mmol/L PBS to remove unentrapped 6-coumarin. All measurements and processing were carried out at room temperature and away from light unless otherwise stated.

S14G-HN-loaded cubosomes (Cubs-S14G-HN) were prepared by using a reverse phase evaporation method. Briefly, GMO, F127 and MAL–PEG–OA were blent at a desired weight ratio (9/0.5/0.5) and dissolved in 2 mL mixed solvent (dichlormethane–ether, 2:8 v/v) to which 0.5 mL of the S14G-HN internal aqueous phase was added within 5 min under an ice-bath sonication (KQ-250DB, Kunshang, China). A thick emulsion was formed, which was then kept in a rotatory evaporator under vacuum in order to remove organic solvent. Then, the gel was resuspended in 1.5 mL of 10 mmol/L phosphate-buffered saline (PBS, pH 7.4) and stirred magnetically for 24 h to hydrate cubosomes. The coarse dispersions were then processed by using a probe sonicator (Scientz Biotechnology Co., Ltd., China) at 200 w energy output for 20 s to form the uniform nanocubosomes. Finally, the unentrapped S14G-HN was separated from the cubosomes by the gel filtration method as described above.

2.3.2. Preparation of OL-modified Cubs

SA (0.5 mg, 8.3 nmol) was thiolated by reacting with a 110:1 molar excess of 2-iminothiolane in 0.15 mol/L sodium borate buffer (pH 8.0) for 45 min, supplemented with 0.1 mmol/L EDTA, as described previously [35]. The product was then applied to a Hitrap™ Desalting column (Amersham Pharmacia Biotech AB, Sweden) and eluted with 0.01 mol/L HEPES (pH 7.0) containing 0.15 mol/L NaCl. The protein fractions were collected, and the introduced thiol groups were determined spectrophotometrically (λ = 412 nm) with Ellman's reagent [36].

Based on SA density at the particle surface, particle size and conjugation efficiency, the coupling protocol or formula parameters were optimized. The milky SA-conjugated Cubs concentration was determined by turbidimetry using a UV2401 spectrophotometer at 350 nm (Shimadzu, Japan). Finally, the OL-modified Cubs were prepared by adding the corresponding quantity of the site-specific biotinylated OL into the SA-coated cubosomes, and the surplus biotinylated OL was removed by a Vivaspin centrifugation filtration device (with a membrane of 300 kDa MWCO, Vivascience, Sartorius) [37].

2.4. Characterization of OL-Cubs

2.4.1. Surface OL and SA densities of OL-Cubs

The average number of SA molecules conjugated per cubosome was determined by sensitive chemiluminescent (CLs) detection [38] with slight modification. The measurement of CLs was performed with a Fluoroskan Ascent (Thermo Electron Corporation), equipped with an incubator and automatic sample assist system. The average number of SA molecules conjugated per cubosome (n) was designated as SA_n. Three types of SA-Cubs with different surface SA density (SA_{54}, SA_{28} and SA_{14}) were acquired through the adjustment of the percent of MAL–PEG–OA to total lipids (to see Appendix A for more details). The average amount of OL coupling on the surface of SA-Cubs was indicated as the B-HRP number, indirectly calculated from the CLs experiments.

2.4.2. Particle size analysis and zeta potential

Particle size distributions of cubosomes were determined by dynamic laser light scattering using the Zeta Potential/Particle Sizer NICOMP™ 380 ZLS (Santa Barbara, CA, USA). Each sample was diluted with ultrapure water, adjusted to a suitable light scattering intensity (300 Hz) and measured at 25 °C in triplicate. Data were collected during 8 min and shown by using average volume-weight size. Following particle size analysis of the cubosomes, the mode was switched from "Size" to "Zeta," the electrode was fitted inside the cuvette, and three measurements of zeta potential were recorded.

2.4.3. Polarizing light microscopy

The coarse samples of SA-Cubs hydrated before and after by PBS were examined under polarizing light microscopy (BK-POLR R&R Polarizing Microscope, Chongqing Optec Instrument Co., Ltd., China) using a λ/4 compensator in order to study the existence of birefringence under crossed polars [39] employing a magnification of 400×. Photomicrographs of these samples were taken at room temperature. The liquid crystalline phases were identified according to the classification established by Rosevear [40].

2.4.4. Cryogenic transmission electron microscopy (cryo-TEM)

The samples (Cubs and OL-Cubs) were prepared in a controlled environment vitrification system. The climate chamber temperature was 25–28 °C, and the relative humidity (about 95%) was kept close to saturation to prevent evaporation from the sample during preparation. A 3 μL droplet of the dispersion was placed on a carbon-coated holey film supported by a copper grid (Quantifoil 1.2/1.3) and gently blotted with filter paper to obtain a thin liquid film (20–400 nm) on the grid. The grid was left on the project part of a cryo-plunger and then rapidly propelled into liquid ethane at approximately 90 K after removal of excess liquid. Excess ethane was removed, and the embedded sample was transferred into a cryoelectron microscope (JEM2010 Cryo-TEM) equipped with a postcolumn energy filter (Gatan GIF 100) using a Gatan-626 Cryo-transfer and workstation. Samples were viewed under low-dose conditions at a constant temperature of around 90–100 K and operated at 200 kV acceleration voltage. The images were recorded digitally with a CCD camera (Gatan-832).

2.4.5. Hemagglutination test

The bioactivity of OL covalently coupled on the surface of SA-Cubs was confirmed by OL-induced agglutination of rat erythrocytes; 200 μL of Cubs or OL-Cubs dilutions (0.5 mg/mL) was incubated with a 200 μL 10% (v/v) suspension of fresh rat erythrocytes in PBS (iso-tonic, pH 7.4) at 37 °C for 30 min. Confirmation of bioactivity was performed by comparing erythroagglutination with that from a positive control (biotin-OL solution) and that from three negative controls (PBS solvent, Cubs and OL-Cubs preincubated with excessive L-fucose). Agglutination was observed and recorded using a photocamera (Olympus BX-50, Japan). The procedure was conducted in triplicate.

2.4.6. Nasal ciliatoxicity

Studies on the nasal ciliatoxicity of cubosomes were conducted using both an in situ toad palate model and an *in vivo* rat nasal mucosa model as described by Jiang et al. [41]. In the toad experiment, the upper palate was exposed and treated with 0.5 mL of cubosomes (2% lipid, w/v) for 0.5 h and then rinsed with physiological saline. The palate was then dissected, the mucocilia were examined under an optical microscope (Olympus, Japan), and the duration of the ciliary oscillation was recorded. In the rat experiment of *in vivo* nasal mucocilia toxicity, 20 μL of cubosomes (1% lipid, w/v) was administered once a day to the unilateral nostril *via* a polyethylene 10 (PE 10) tube attached to a microliter syringe. Cubosomes were administered for 6 days. The rats were sacrificed 24 h after the last administration, the nasal mucosa was peeled off, and the mucocilia were examined under a scanning electron microscope (SEM) (JSM-T300, Japan). Physiological saline and 1% (w/v) sodium deoxycholate (a nasal ciliatoxic agent, 1% solution) were used as the negative and positive control, respectively, and the untreated nostril was also used as a negative control.

2.5. Encapsulation efficiency, loading capacity and in vitro release of 6-coumarin or S14G-HN from OL-Cubs

To determine the 6-coumarin or S14G-HN content, Cubs and OL-Cubs were dissolved in methanol and 6-coumarin or S14G-HN was determined by HPLC analysis [19,42,43]. The analyses were performed in triplicate. The encapsulation efficiency (EE) and drug loading capacity (DLC) were calculated by the following equations:

$$\text{EE}\ (\%) = \frac{\text{encapsulated drug in cubosomes}}{\text{total drug in cubosomes}} \times 100\%$$

$$\text{DLC}\ (\%) = \frac{\text{amount of drug in cubosomes}}{\text{cubosomes weight}} \times 100\%$$

Since 6-coumarin is lipophilic and easily absorbed to its containers at high concentration, 10% (v/v) ethanol–PBS (pH 7.4 and pH 4.0) that contributed to fully meeting the "sink" condition of 6-coumarin was used as release medium with a dialysis bag (MWCO: 3500 Da). The entire system was kept at 37 °C with shaking at 180 rpm. Samples were withdrawn from the medium, and the same volume of fresh dissolution medium at 37 °C was added. The amount of 6-coumarin in each of the release samples was analyzed by the HPLC method described above. Care was taken to protect the samples from light throughout the experimental procedure.

In vitro release of S14G-HN from cubosomes was conducted in a glass-stopped tube, and S14G-HN-loaded cubosomes were added into a dialysis bag (MWCO: 14,000 Da) and then incubated in the medium of artificial nasal fluid (ANF, pH 6.5) [44] or pH 7.4 PBS at 37 °C within a rotary shaker (180 r/min). Samples were removed from the tube at appropriate time intervals, replaced with an equal volume of isothermal fresh media and then measured by the HPLC method as described [43] to determine the amount of S14G-HN.

2.6. Evaluation of systemic absorption and brain delivery of 6-coumarin-loaded OL-Cubs

2.6.1. Animal experiments

To evaluate the brain uptake of OL-Cubs and Cubs, 6-coumarin was incorporated into three cubosomes, Cubs (unmodified), OL_{50}-Cubs (the average number of OL per cubosome was about 50) and OL_{150}-Cubs, and administered to 16 rats, respectively. Each animal received a total of about 0.2 mg (1.0 mg/kg) of cubosomes in 20 μL (10 μL each nostril) of 10 mmol/L PBS (pH 7.4). For intranasal administration, conscious animals were fixed in the supine position, and the preparations were given at the openings of the nostrils using a polyethylene 10 (PE 10) tube attached to a microliter syringe. The procedure lasted about 2 min, allowing the rats to inhale the preparations.

At different time intervals (i.e., 0.5, 2, 4 and 8 h) after administration, the animals (four animals each point) were anesthetized with ether, and blood samples (about 1 mL) were collected from the ocular fundus vein. The rats were subsequently euthanized, and tissue samples were collected following decapitation. The skulls were cut open, and brain tissue samples were excised from three regions, the cerebrum (CR), cerebellum (CL) and olfactory bulb (OB), which were weighed and stored at −20 °C until assayed.

2.6.2. Analytical procedure and data analysis

The brain and blood samples were treated, and chromatographic analysis was performed as our previously published study [19,20]. The concentration data were dose-normalized and plotted as drug concentration–time curves for the blood and brain tissues. The area under the concentration–time curve ($AUC_{0\to t}$) was calculated by the trapezoidal rule, and the variance for the $AUC_{0\to t}$ was estimated by the method of Yuan [45]. The brain/blood $AUC_{0\to t}$ ratios for coumarin carried by OL-Cubs and unmodified cubosomes were calculated to evaluate the drug targeting efficiency (DTE) [46].

Statistical analyses were performed using SPSS 12.0 software. Means are shown with SD unpaired Student's *t*-tests were performed to compare OL-modified Cubs *versus* unmodified cubosomes using a 95% confidence level.

2.7. Neuroprotection effects of the S14G-HN formulation on $A\beta_{25-35}$-induced cholinergic inhibition

2.7.1. In vivo model for cholinergic inhibition

$A\beta_{25-35}$ was dissolved in sterile artificial cerebrospinal fluid (ACSF, pH 7.3) at a concentration of 2 g/L, incubated in a capped vial at 37 °C for 7 days to form aggregated according to previous reports [47–49] and stored at −20 °C until further use.

A total of seventy SD rats were randomly divided into seven groups (Table 1) and anesthetized with 10% hydral (250 mg/kg, i.p) and fixed in a David Krof stereotaxic apparatus. After a midline incision, holes were drilled bilaterally in the skull overlying the hippocampal area. $A\beta_{25-35}$ (2 g/L, 5 μL/side) were slowly injected into the hippocampal area (CA1–CA3 in Fig. 2A, aimed at 3.0 mm posterior to the bregma, 2.0 mm lateral to the midline and 3.2 mm ventral from the skull surface) as referred to the atlas of Paxinos [50] by 10-μL Hamilton syringe with a 2-mm, 26-gauge needle (Hamilton, USA). The needle was kept 3 min before withdrawn, with the denture powder to fill the pinholes, then the incision was sutured and disinfected, and the rat was not conventionally bred until fully awake. Sham-operated animals were injected with the same volume of solvent (ACSF). To verify

Table 1
Groups and treatments.

Groups	Treatments
Sham control	i.n. 0.1 mL/kg saline, 10 μL/nostril/day for 12 day
AD control	i.n. 0.1 mL/kg saline, 10 μL/nostril/day for 12 days
Blank OL-Cubs	i.n. 1.5 mg/kg blank OL-Cubs, 10 μL/nostril/day for 12 days
Cubs-S14G-HN (2.5)	i.n. 2.5 μg/kg S14G-HN carried by Cubs, 10 μL/nostril/day for 12 days
Cubs-S14G-HN (7.5)	i.n. 7.5 μg/kg S14G-HN carried by Cubs, 10 μL/nostril/day for 12 days
OL-Cubs-S14G-HN (2.5)	i.n. 2.5 μg/kg S14G-HN carried by OL-Cubs, 10 μL/nostril/day for 12 days
OL-Cubs-S14G-HN (7.5)	i.n. 7.5 vg/kg S14G-HN carried by OL-Cubs, 10 μL/nostril/day for 12 days

the locus of the injection, several rats were injected intrahippocampally with the same volume of Indian ink.

2.7.2. Experimental protocol

After the intrahippocampal injection, the following scheme was carried out as shown in Fig. 2D. To induce amnesia by Aβ, the rats treated with $A\beta_{25-35}$ were conventionally bred for 14 days before administration. Intranasal administration of Cubs-S14G-HN, OL-Cubs-S14G-HN and blank OL-Cubs was carried out according to the plan (Table 1). Sham control and AD ($A\beta_{25-35}$) control animals received intranasal administration of normal saline (NS). Seven days later after recovery, spatial working memory performance was evaluated, by monitoring spontaneous alternation behavior in the Morris water maze test, 1 h following drug administration for 5 days. The behavioral test procedures were carried out as described previously [18]. Briefly, the rats were placed in a circular black pool 180 cm in diameter and 30 cm deep, equipped with a 9-cm platform 1.5 cm below the surface of the water at about 30 °C in the middle of a quadrant. A high-resolution exview HAD camera (Shenzhen Hong Tianzhi Electronics Co. Ltd., Shenzhen, China) was suspended over the center of the pool, its images being monitored by a video-tracking system [Morris Water Maze Video Analysis System (DigBeh-MM), Shanghai Jiliang Software Technology Co. Ltd., Shanghai, China]. On the first 4 days, the rats were tested four times daily being put into the water from the starting points which divided the pool into four quadrants with a daily-different-random sequences. The cutoff time for the latency to reach the platform was 90 s; if one animal did not find the platform after 90 s, it was then placed on the platform for 30 s. The latency to reach the platform was recorded for each rat, and its declines over days of training reflected learning and memory. On the fifth day, each rat was given two single probe tests with the platform removed, where the rat was placed in water from the two starting points farther away from the platform by order, the average number of cross times recorded.

2.7.3. Measurements of acetylcholinesterase activity

It was proved that intrahippocampal injection of $A\beta_{25-35}$ destroyed cholinergic nerve in the hippocampus in rats [51,52]. Hereto, in this study, we measured acetylcholinesterase activity in rat hippocampus at the termination of the behavioral experiments using the method described by Li et al. [53]. Comparisons were made among Sham controls, AD controls, $A\beta_{25-35}$ + blank OL-Cubs-treated, $A\beta_{25-35}$ + Cubs-S14G-HN and $A\beta_{25-35}$ + OL-Cubs-S14G-HN-treated ones.

2.7.4. Statistical analysis

For multiple-group comparison, the data were analyzed by one-way analysis of variance (ANOVA). When *P*-values by ANOVA were lower than 0.05, Bonferroni *post hoc* test was carried out. Specific comparison between groups was carried out with a two-sided unpaired Student's *t*-test, and differences were considered statistically significant at $P < 0.05$.

3. Results and discussion

3.1. OL-Cubs preparation and characterization

3.1.1. Preparation of OL-modified Cubs

SA is a tetrameric protein with the ability to bind four biotin molecules and derivative forms of biotin with exceptionally high affinity; the biotin-OL was thereby coupled onto the SA-modified cubosomes by a non-covalent (biotin–SA) method. Both coupling of maleimide to the thiol group and SA to biotin are highly specific, simple and reproducible. These reactions can take place under mild conditions. These traits are of significant importance in preserving the activity of other functional groups and to allow optimal target recognition of OL. Considering the flexibility of targeting, the ligand might influence its receptor binding capacity [54]. A molar ratio of SA/2-iminothiolane at 1:110 was optimized to provide approximately one thiol group per SA. The preparation protocol parameters were also optimized with the ratio of MAL–PEG–OA to total lipids (GMO + F127) of around 3% (mol/mol), thiolated SA/MAL–PEG–OA 1:50 and a conjugation time of 8 h.

3.1.2. Surface OL and SA densities of OL-Cubs

CLs is a highly sensitive detection method widely used in immunoassay, due to its simple optical system and low background nature. This method is uniquely suited to detect amino acids, peptides and DNA. According to the specificity results (Fig. 3A), the CLs intensity of SA-Cubs containing little free SA unconjugated to PEGylated cubosome particles (before eluting) was lower than that of SA-Cubs (upon eluting), because the former left less B-HRP than the latter, while SA-unmodified Cubs such as PEGylated Cubs and common Cubs did not affect B-HRP and showed the strongest signal. These findings confirmed the conjugation of SA with the PEGylated Cubs. Moreover, no effect of lipid concentration on CLs detection was observed (Fig. 3B) when the lipids were less than 5% (m/v). The CLs peak signal *versus* the B-HRP concentration curve (Fig. 3C) proved to be linear. The regression line equation calculated by the least-squares method was $A = 15889C - 703.51$ with a correlation coefficient of $r = 0.999\ 5$ (ranging from 0.25 to 50 ng/mL). Thus, the CLs method was specific, sensitive and suitable for the detection of surface-modified SA. It is known that SA, a tetrameric protein, has the ability to bind four molecules of biotin and derivatized forms of biotin with exceptionally high affinity [55]. As biotin-OL was orientedly synthesized from the beginning of biotin-Tyr synthesis, the single biotin molecule was connected to the N-terminal of OL to prepare mono-biotinylated OL. Therefore, the OL number per cubosome connected with the added biotin-OL for high efficiency coupling of SA to biotin was also obtained.

3.1.3. Cryo-TEM, particle sizing and drug loading

The Cryo-TEM and polarizing light microscopy results confirmed the bi-continuous liquid crystalline phase and indicated "honeycomb" or multivesicular in shape with clearly visible cell units (Fig. 4). Further characterization of internal structure will be performed by Synchrotron Radiation Small Angle X-ray Scattering. Upon encapsulation of 6-coumarin, the Cubs and OL-Cubs had similar features such as average diameters, zeta potential and entrapping efficiency (Table 2), suggesting that conjugation of SA and biotin-OL had no significant influence on the properties of Cubs. However, upon S14G-HN incorporation, a slight decrease in diameter and potential was observed following their conjugation

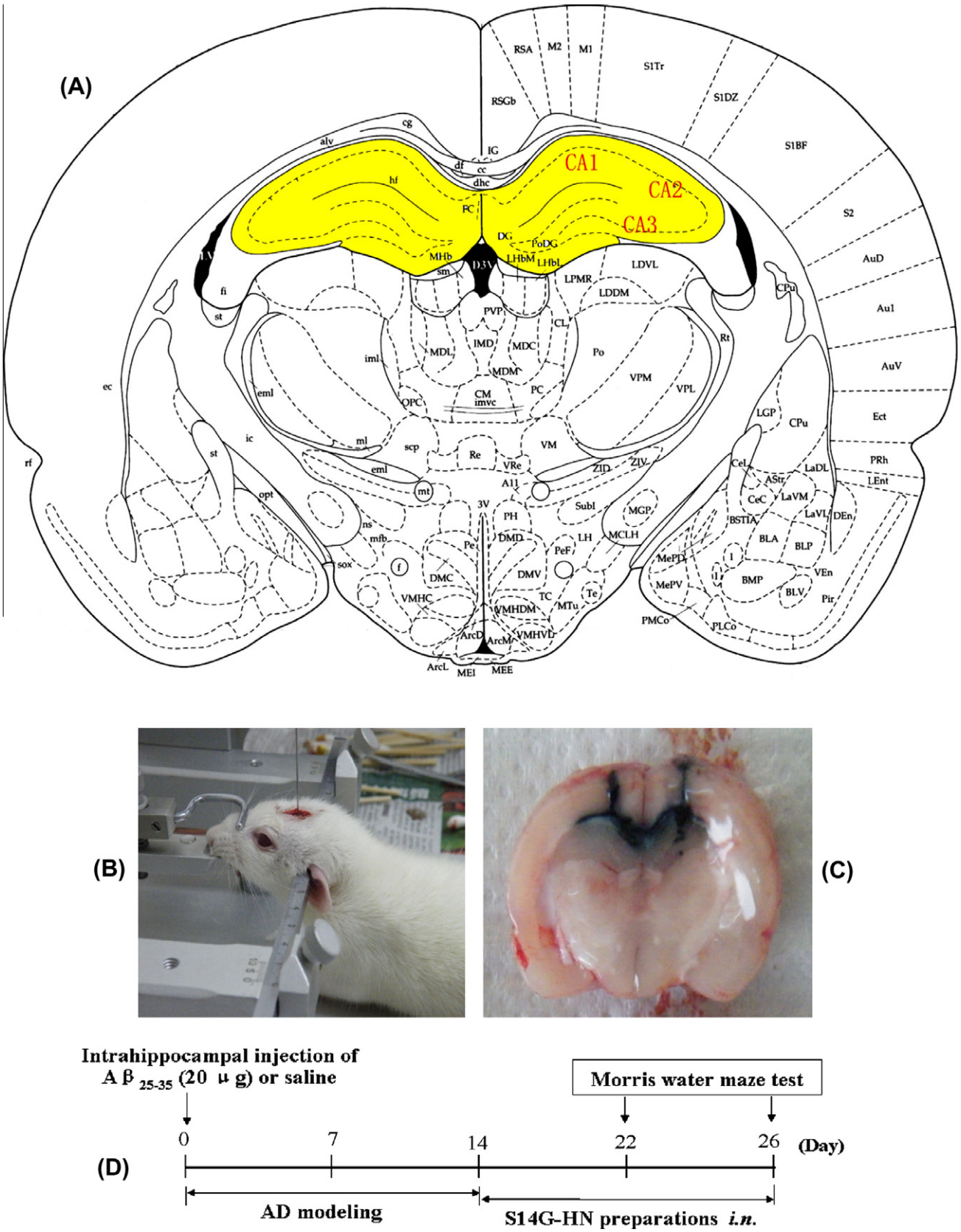

Fig. 2. Schematic representation showing the intrahippocampal injection and Morris water maze test schedule. (A) the hippocampal area (yellow area) referred from the atlas of Paxinos; (B) the animals were fixed and injected intrahippocampally in a stereotaxic apparatus; (C) the area injected with Indian ink (black area); and (D) schedule for intrahippocampal injection and Morris water maze test. (For interpretation of the references to color in this figure legend, the reader is referred to the web version of this article.)

to OL, finding that the OL-Cubs-S14G-HN was 100–120 nm in size and −14.05 mV in potential. It might be related to the embedding of hydrophobic peptide chain of S14G-HN and MAL–PEG–OA that changes the curvature of the lipid membrane, and then the cubic vesicles self-assembled downsized. The reverse phase evaporation process resulted in a total drug load of 0.85% (w/w) of S14G-HN inside the Cubs with a relative high encapsulation efficiency of 65.97%. S14G-HN is a highly potent HN derivative, which structure has many hydrophobic amino acids, such as leucine, isoleucine and alanine. This might contribute to the entrapment of S14G-HN into lipid bilayer of the cubosomes.

3.1.4. Hemagglutination test and in vitro release of 6-coumarin or S14G-HN from OL-Cubs

Hemagglutination testing showed that OL molecules retained their carbohydrate binding bioactivity after coupling on the surface of cubosomes (indicated by black arrows in Fig. 5).

In vitro release study conducted in 10% ethanol–PBS (pH 4.0) and 10% ethanol–PBS (pH 7.4) showed that almost all the free form of 6-coumarin could diffuse through the dialysis membrane within 4 h and no more than 2% of 6-coumarin was released from OL-Cubs after a 24 h incubation period (Supplementary data, Fig. S3). This lack of release indicated that 6-coumarin was an appropriate fluorescent probe, and the fluorescence signal detected in the blood and brain tissue samples was mainly attributed to 6-coumarin encapsulated in the cubosomes; the qualitative results (Supplementary data, Fig. S5) indicated that there were stronger green fluorescent signals like stars in the brain slices and also proved it.

The *in vitro* release of S14G-HN from Cubs was investigated in pH 6.5 ANF and pH 7.4 PBS, whose results shown that approximately 32% S14G-HN was released from Cubs in pH 6.5 during 12 h incubation, and 31% released in pH 7.4 during the same time (Supplementary data, Fig. S4), which suggested that most drugs were to remain in the cubosomes when absorb upon transnasal administration.

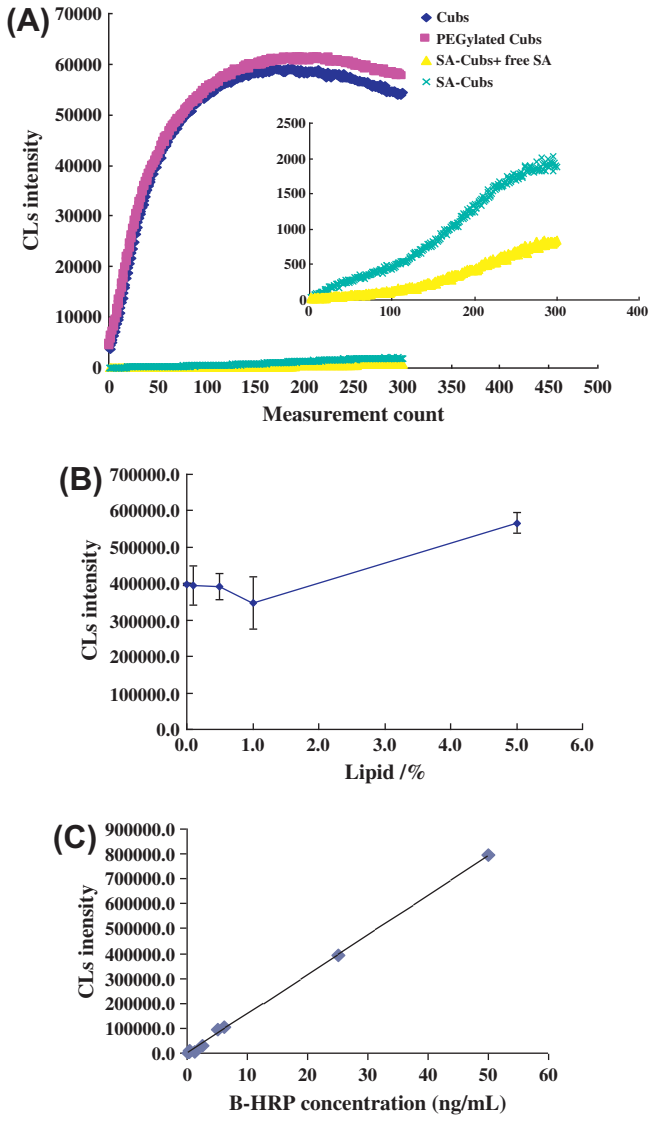

Fig. 3. The empirical method of CLs detection. (A) Specificity of the CLs method, (B) effect of lipid concentration on CLs detection ($n = 3$) and (C) calibration curve of CLs signal *versus* B-HRP concentration. (For interpretation of the references to color in this figure legend, the reader is referred to the web version of this article.)

3.2. Nasal ciliatoxicity

Since ciliary movement is a major indication of mucociliary clearance in the upper airways, it is important to evaluate the influence of nasal preparations on ciliary morphology and movement. Optical microscopic observation of toad palate showed that there were a great number of cilia with a fast beating rate on the edge of the mucosa treated with both OL-Cubs and Cubs for 0.5 h (Supplementary data, Fig. S6.A–D) and that the duration of ciliary movement lasted for 9.25 h and 8.03 h for the OL-Cubs and Cubs treated mucosa, respectively. These values were comparable with those of the negative control (10.82 h) and much longer than those

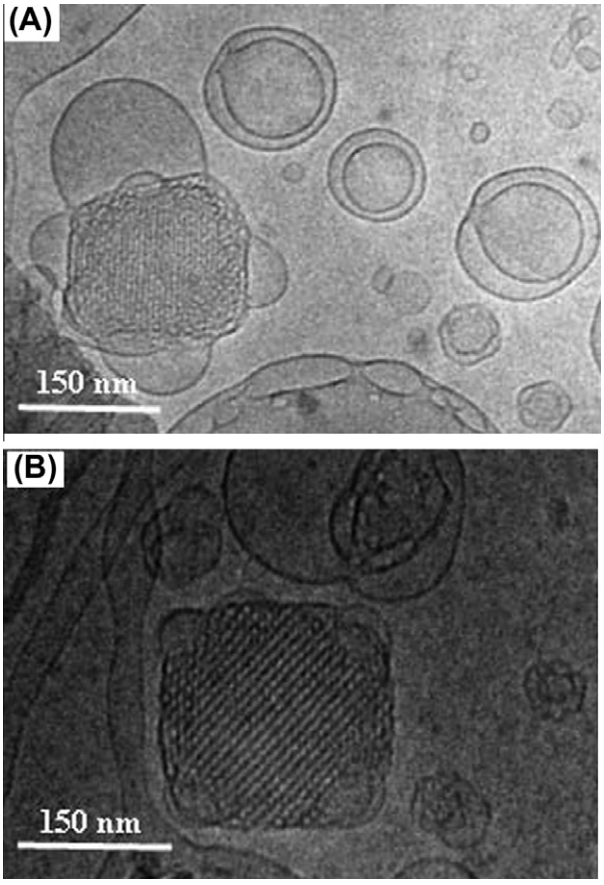

Fig. 4. Cryo-TEM image of Cubs (A) and OL-Cubs (B) encapsulating 6-coumarin (bar 150 nm).

Table 2
Characterization of 6-coumarin or S14G-HN-loaded Cubs, OL_{50}-Cubs and OL_{150}-Cubs (Mean ± SD, $n = 3$).

	Cubs	OL_{50}-Cubs	OL_{150}-Cubs	Cubs-S14G-HN	OL_{150}-Cubs-S14G-HN
Particle size (nm)	177.3 ± 33.4	175.5 ± 45.6	187.7 ± 36.8	136.7 ± 42.5	92.8 ± 38.2
Zeta potential (mV)	−16.7 ± 3.0	−19.4 ± 2.5	−19.9 ± 2.7	−8.74 ± 0.65	−14.1 ± 1.3
EE (%)	74.12 ± 1.4	75.78 ± 2.1	73.02 ± 2.4	65.97 ± 3.70	58.93 ± 4.50
DLC (%)	0.15 ± 0.01	0.13 ± 0.02	0.12 ± 0.02	0.85 ± 0.04	0.80 ± 0.05

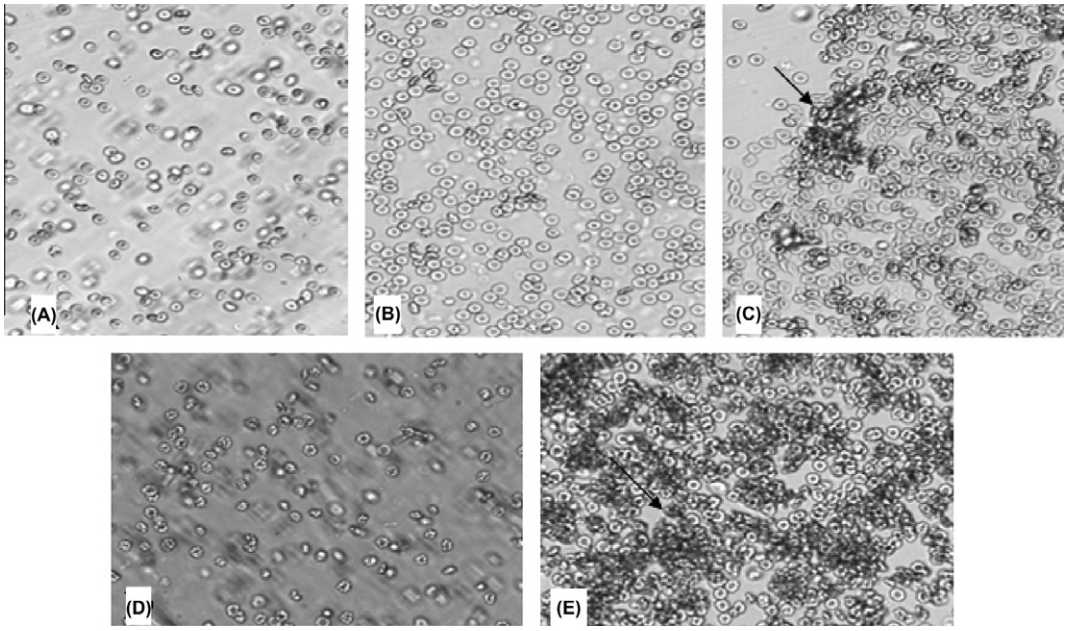

Fig. 5. Microphotographs of fresh rat erythrocytes following incubation with Cubs and OL-Cubs. (A) 200 μL 10% (v/v) suspension of fresh rat erythrocytes + 200 μL PBS (isotonic, 10 mmol/L, pH 7.4) incubated at 37 for 30 min; (B) 200 μL 10% suspension of fresh rat erythrocytes + 200 μL Cubs (0.5 mg/mL) at 37 °C for 30 min; (C) 200 μL 10% suspension of fresh rat erythrocytes + 200 μL OL-Cubs (0.5 mg/ml) at 37 °C for 30 min; (D) 150 μL OL-Cubs (0.5 mg/mL) + 50 μL L-fucose (100 mmol/L) + 200 μL 10% suspension of fresh rat erythrocytes at 37 °C for 30 min; (E) 200 μL 10% suspension of fresh rat erythrocytes + 200 μL biotin-OL solution (0.1 mg/mL) at 37 °C for 30 min.

of the positive control (only 15 min). The data were consistent with the results shown by SEM in the *in vivo* rat nasal mucosa model (Supplementary data, Fig. S6.E–H). In the negative control, the morphology and integrity of the cilia on the nasal mucosa, which was not affected by the administration of physiological saline, were dense, regular and intact. After intranasal administration of OL-Cubs and Cubs, no visible change (or a similar change to that with saline was visualized) in the morphology and integrity of the cilia was observed, while 1% sodium deoxycholate (positive control) caused severe damage with irregular or absent cilia and abundant mucus extrusion observed. These results suggest that the nasal ciliatoxicity of OL-Cubs and Cubs was negligible.

3.3. Evaluation of systemic absorption and brain delivery of 6-coumarin-loaded OL-Cubs

The systemic adsorption of 6-coumarin associated with both OL-Cubs and Cubs exhibited similar concentration–time profiles, except that the maximum blood concentration of OL-Cubs was reached 1 h earlier than that of the unmodified cubosomes ($T_{max,\ Cubs}$, 2 h; $T_{max,\ OL50\text{-}Cubs}$, 1 h; $T_{max,\ OL150\text{-}Cubs}$, 0.5 h). This evidence suggested that OL on the surface of cubosomes could accelerate access of drugs carried by cubosomes to the blood. However, according to Fig. 6, OL modification did not increase the delivery of cubosomes to blood. The little contact time that the non-coated Cubs had at the nasal mucous membrane might be one reason for this finding. Most of the cubosomes were swallowed and adsorbed into blood through the gastrointestinal tract mucosa following intranasal administration, so the peak time for Cubs lagged behind. In general, the absorbing velocity of nasal mucous membrane is more rapid than that of gastrointestinal tract mucosa; however, there may be no discrepancy in the extent of absorption. In addition, as the olfactory area of rats spreads about 50% of the total area of nasal mucosa, the non-specific adsorption of OL with the respiratory mucosa was conducive to the penetration. Therefore, surface modification of the cubosomes with OL led to more rapid delivery but no enhancement of drugs in the systemic circulation.

A significant increase in the DTE of OL_{150}-Cubs was observed (1.99, 3.46 and 1.66 times in the OB, CR and CL, respectively), with an increase of 2.61 times in OL_{50}-Cubs in the CR compared with that of 6-coumarin incorporated in unmodified Cubs (Fig. 6). According to Fig. 6, the AUC of OB and AUC ratio (OB/blood) of OL-modified cubosomes were both higher than those of unmodified cubosomes. OL functionalization facilitated the adsorption of coumarin entrapped in cubosomes in the brain, which might have resulted from conjugating OL inducing close contact of the cubosomes with the mucosal cells to produce a stronger penetration with rapid extracellular transport [4,56]. OL might also trigger or facilitate the active transport of cubosomes through the nasal mucosa, especially the olfactory mucosa. On the other hand, OL engineering might facilitate the direct transport of some cubosomes to the brain tissues through the trigeminal nerves at the respiratory epithelium [57]. As OL was found by Lai's group only recently [20], the trigeminal neural and/or other transport mechanisms still need further investigation. Whichever pathway is involved, OL

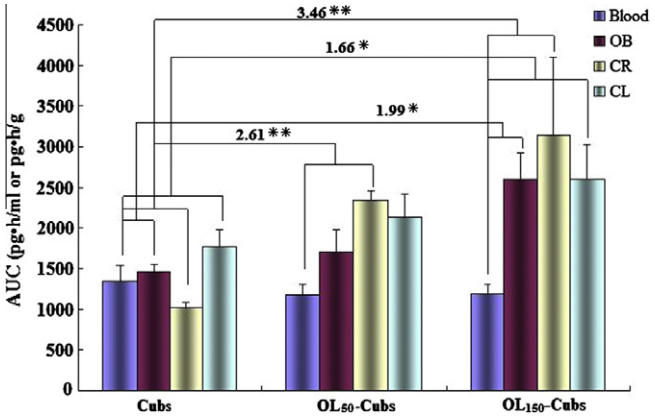

Fig. 6. AUC column diagram of 6-coumarin in the blood, OB, CR and CL following an intranasal administration of coumarin-loaded Cubs, OL_{50}-Cubs and OL_{150}-Cubs in rats at the dose of 5.0 μg/kg of 6-coumarin ($n = 4$). Statistically significant difference by one-tailed Student's t-test when compared to corresponding value of Cubs ($^{*}P < 0.05$, $^{**}P < 0.01$). (For interpretation of the references to color in this figure legend, the reader is referred to the web version of this article.)

modification contributed to promoting drug transport to the brain. The accumulation of coumarin in the brain was faster and greater when OL was denser.

As indicated in this study, OL can facilitate the access of drugs carried by cubosomes to the brain. However, the enhanced absorption effect of our small-peptide OL engineering was not in excess of some previously reported protein-lectin systems such as WGA [19,58] and UEA I [21]. There were three major factors to take into account. Firstly, the effect varied depending on the kind of lectin selected, since different targeting tissues presented different types and intensities of carbohydrates. Secondly, the effect relied on the intensity and binding activity of lectins conjugated on the surface of cubosomes. Thirdly, small peptides are more liable to be degraded in the internal milieu than proteins. Therefore, further research will be conducted to determine the influence of several parameters on the brain uptake effect, such as the category and intensity of coating lectins, the PEG spacer length and the core materials.

3.4. Neuroprotection effects of the S14G-HN formulation on $A\beta_{25-35}$-induced cholinergic inhibition

Aβ injection model used in the previous studies [30,59] is a simple and convenient model. To verify that injection was carried out properly, we checked the position using ink. Distribution of the injected ink throughout both sides of the hippocampus region (CA1–CA3) was confirmed (Fig. 2C).

As the results shown in Fig. 7A, rats treated with $A\beta_{25-35}$ exhibited disruption of learning and memory in the water maze, and significantly longer latencies than Sham control. Intranasal application improved the spatial memory in a dose-dependent manner: 7.5 μg/kg of S14G-HN loaded by Cubs apparently shortened the escape latency on days 2, 3 and 4, while the effect of 2.5 μg/kg was not obvious. But in the case of drug carried by OL-

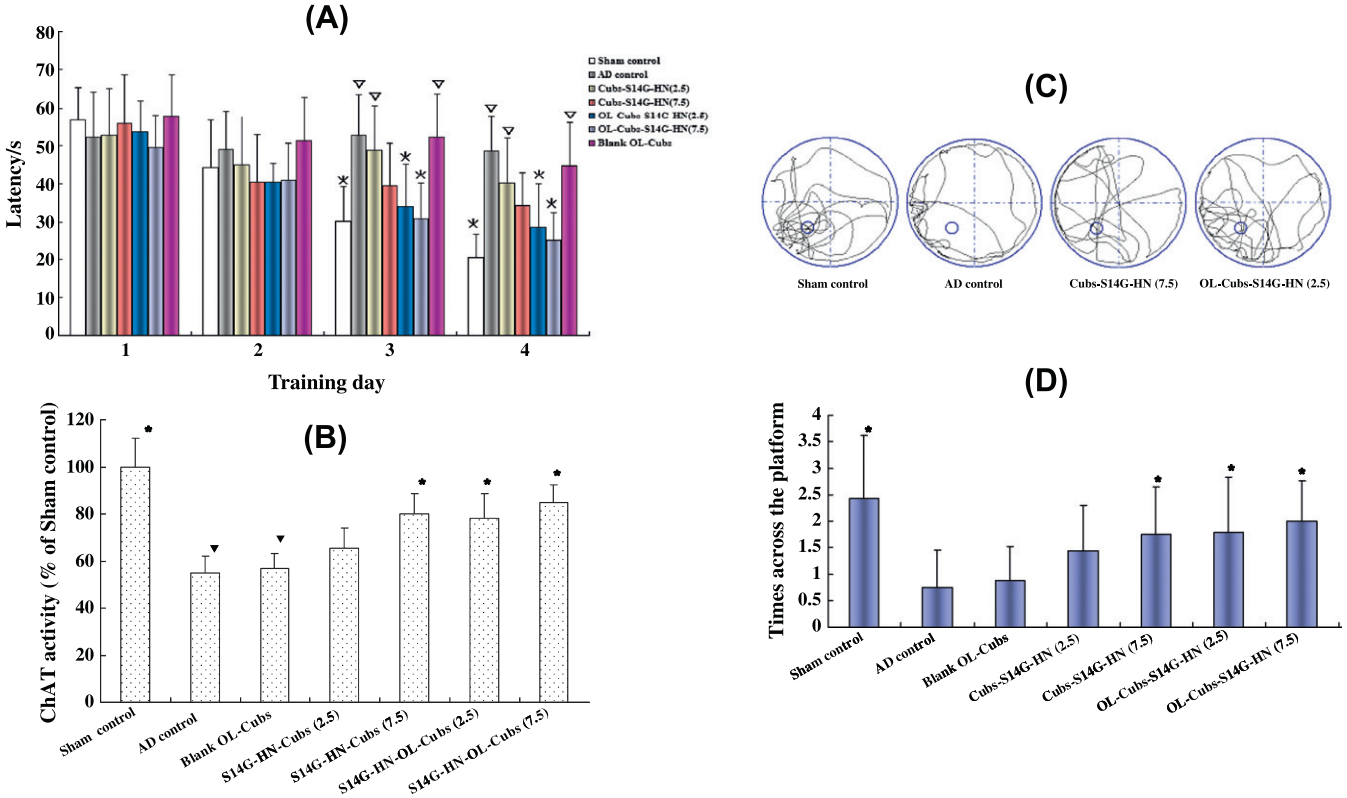

Fig. 7. Neuroprotection effects of intranasal administration of S14G-HN preparations on the impairment of water maze learning in rats with $A\beta_{25-35}$-induced lesions. (A) Training began after 14 days of recovering and following 7 daily drug applications. (B) Acetylcholinesterase activity in $A\beta_{25-35}$-treated rats. Results were calibrated against sham control (100%); (C) swim paths; and (D) the number of times crossed the area where the platform had been located. Data represented the mean ± SEM. Sham control, given artificial cerebrospinal fluid instead of $A\beta_{25-35}$ and received daily applied NS; $A\beta_{25-35}$ control, daily applied NS; Cubs-S14G-HN (2.5), intranasal administration of S14G-HN-loaded Cubs at the dose of 2.5 μg/kg S14G-HN; Cubs-S14G-HN (7.5), intranasal administration of S14G-HN-loaded Cubs at the dose of 7.5 μg/kg S14G-HN; OL-Cubs-S14G-HN (2.5) and OL-Cubs-S14G-HN(7.5), intranasal administration of OL-modified S14G-HN-loaded Cubs at the dose of 2.5 and 7.5 μg/kg S14G-HN, respectively. $^{*}P < 0.05$, significantly different compared to the $A\beta_{25-35}$ control; $^{\nabla}P < 0.05$, significantly different compared to the Sham control ($n = 10$). (For interpretation of the references to color in this figure legend, the reader is referred to the web version of this article.)

Cubs, significant improvement was observed at the dose of 2.5 μg/kg. The same results were presented from the probe tests on the fifth day. AD control animals crossed the area where the platform had been located during training, significantly fewer times than Sham controls. This reduction in the number of times was ameliorated by intranasal administration of 7.5 μg/kg of S14G-HN entrapped in Cubs or 2.5 μg/kg of S14G-HN carried by OL-Cubs shown a similar significant improvement (Fig. 7D), the representative swim path for each group is presented in Fig. 7C. Compared with AD controls whose animals swam around the pool and scarcely crossed the platform, OL-Cubs-S14G-HN-treated animals swam more in the quadrant where the platform located. These outcomes were further confirmed by acetylcholinesterase activity in hippocampus of rats at the termination of the experiment, where $A\beta_{25-35}$ animals showed a 45% reduction, intranasal administration of Cubs-S14G-HN alleviated the reduction in a dose-dependent manner, and OL-Cubs-S14G-HN (at dose of 2.5 μg/kg) treatment resulted in increased cholinergic activity remarkable from Sham control values (Fig. 7B).

The improvement in brain drug delivery of OL modification was consistent with the brain distribution results above. OL functionalization increased the absorption of 6-coumarin and S14G-HN carried by cubosomes in the brain, which might have resulted from the fact that the conjugation OL induced strong mucoadhesion, or a close contact of the cubosomes with the mucosal cells so as to produce a stronger penetration. Also, the olfactory mucosa played a vital role in the transport of drugs into the brain and cerebrospinal fluid [60]. Thus, it was possible that the affinity of OL-Cubs to the olfactory mucosa contributed to ameliorate learning impairment and enhance ChAT activity in the hippocampus. However, it was not clear yet whether intact cubosomes were absorbed into the brain and the direct evidences need to be presented; it was also hard to tell that the virtue was from S14G-HN remained on the cubosomes or from that already released from the cubosomes. Nevertheless, the improvement in brain drug delivery following intranasal application of OL-Cubs was a fact, suggesting that OL-Cubs might offer a potential brain delivery system especially for peptide and protein drugs.

4. Conclusion

Since most peptides and proteins with considerable potential in the treatment of brain diseases are susceptible to enzymes *in vivo* and hold a poor ability to cross the BBB, the current work succeeded in developing a protocol for surface engineering of PEGylated cubosomes with functional molecules, mediating S14G-HN transport into the brain and ameliorating learning impairment in AD rats. It should be noted that OL is the smallest lectin known and has extremely low immunogenicity and potential advantages over large sized lectins for drug delivery. As a homing molecule, OL-bearing cubosomes might provide a novel effective and noninvasive technique for brain drug delivery, especially for biotech drugs such as peptides, proteins and DNA.

Acknowledgements

The authors kindly thank Danisco (China) Co., Ltd. for generously providing the pharma 19 GMO and Lecturer Kunpeng Li from the Laboratory of Bio-Electron Microscopy School of Life Sciences, Sun Yat-sen University, who carried out Cryo-TEM and Prof. Ling Qi for TEM analysis. Financial support from the National Basic Research Program of China (973 Program) 2007CB935800 and 2010CB529806, National Science and Technology Major Project 2009ZX09310-006 and the National Natural Science Foundation of China (No. 30801439) is gratefully acknowledged.

Appendix A. Supplementary material

Supplementary data associated with this article can be found, in the online version, at doi:10.1016/j.ejpb.2011.10.012.

References

[1] D. Lindholm, P. Carroll, G. Tzimagiorgis, H. Thoenen, Autocrine–paracrine regulation of hippocampal neuron survival by IGF-1 and the neurotrophins BDNF, NT-3 and NT-4, Eur. J. Neurosci. 8 (1996) 1452–1460.
[2] Y. Hashimoto, T. Niikura, Y. Ito, H. Sudo, M. Hata, E. Arakawa, Y. Abe, Y. Kita, I. Nishimoto, Detailed characterization of neuroprotection by a rescue factor humanin against various Alzheimer's disease-relevant insults, J. Neurosci. 21 (2001) 9235–9245.
[3] H.B. Wu, K.L. Hu, X.G. Jiang, From nose to brain: understanding transport capacity and transport rate of drugs, Expert Opin. Drug Deliv. 5 (2008) 1159–1168.
[4] S.V. Dhuria, L.R. Hanson, W.H. Frey II, Intranasal delivery to the central nervous system: mechanisms and experimental considerations, J. Pharm. Sci. 99 (2010) 1654–1673.
[5] D.A. Christian, S. Cai, D.M. Bowen, Y. Kim, J.D. Pajerowski, D.E. Discher, Polymersome carriers: from self-assembly to siRNA and protein therapeutics, Eur. J. Pharm. Biopharm. 71 (2009) 463–474.
[6] C.M. Lehr, Lectin-mediated drug delivery: the second generation of bioadhesives, J. Control. Release 65 (2000) 19–29.
[7] D. Bei, J.N. Meng, Bi-Botti C. Youan, Engineering nanomedicines for improved melanoma therapy: progress and promises, Nanomedicine 5 (2010) 1385–1399.
[8] Y. Sadhale, J.C. Shah, Stabilization of insulin against agitation-induced aggregation by the GMO cubic phase gel, Int. J. Pharm. 191 (1999) 51–64.
[9] Y. Sadhale, J.C. Shah, Biological activity of insulin in GMO gels and the effect of agitation, Int. J. Pharm. 191 (1999) 65–74.
[10] E.M. Landau, J.P. Rosenbusch, Lipidic cubic phases: a novel concept for the crystallization of membrane proteins, Proc. Natl. Acad. Sci. USA 93 (1996) 14532–14535.
[11] J.R. Giorgione, Z. Huang, R.M. Epand, Increased activation of protein kinase C with cubic phase lipid compared with liposomes, Biochemistry 37 (1998) 2384–2392.
[12] J. Barauskas, M. Johnsson, F. Tiberg, Self-assembled lipid superstructures: beyond vesicles and liposomes, Nano Lett. 5 (2005) 1615–1619.
[13] S.B. Rizwan, B.J. Boyd, T. Rades, S. Hook, Bicontinuous cubic liquid crystals as sustained delivery systems for peptides and proteins, Expert Opin. Drug Deliv. 7 (2010) 1133–1144.
[14] J.C. Shah, Y. Sadhale, D.M. Chilukuri, Cubic phase gels as drug delivery systems, Adv. Drug Deliv. Rev. 47 (2001) 229–250.
[15] G. Garg, S. Saraf, S. Saraf, Cubosomes: an overview, Biol. Pharm. Bull. 30 (2007) 350–353.
[16] S. B Rizwan, D. Assmus, A. Boehnke, T. Hanley, B.J. Boyd, T. Rades, S. Hook, Preparation of phytantriol cubosomes by solvent precursor dilution for the delivery of protein vaccines, Eur. J. Pharm. Biopharm. 79 (2011) 15–22.
[17] T-.H. Nguyen, T. Hanley, C.J.H. Porter, B.J. Boyd, Nanostructured liquid crystalline particles provide long duration sustained-release effect for a poorly water soluble drug after oral administration, J. Control. Release 153 (2011) 180–186.
[18] Y.S. Yin, D.W. Chen, M.X. Qiao, Z. Lu, H.Y. Hu, Preparation and evaluation of lectin-conjugated PLGA nanoparticles for oral delivery of thymopentin, J. Control. Release 116 (2006) 337–345.
[19] X.L. Gao, W.X. Tao, W. Lu, Q.Z. Zhang, Y. Zhang, X.G. Jiang, S. Fu, Lectin-conjugated PEG–PLA nanoparticles: preparation and brain delivery after intranasal administration, Biomaterials 27 (2006) 3482–3490.
[20] X.L. Gao, B.X. Wu, Q.Z. Zhang, J. Chen, J.H. Zhu, W.W. Zhang, Z.X. Rong, H.Z. Chen, X.G. Jiang, Brain delivery of vasoactive intestinal peptide enhanced with the nanoparticles conjugated with wheat germ agglutinin following intranasal administration, J. Control. Release 121 (2007) 156–167.
[21] X.L. Gao, J. Chen, W.X. Tao, J.H. Zhu, Q.Z. Zhang, H.Z. Chen, X.G. Jiang, UEA I-bearing nanoparticles for brain delivery following intranasal administration, Int. J. Pharm. 340 (2007) 207–215.
[22] J.X. Li, H.B. Wu, J. Hong, X.Q. Xu, H.L. Yang, B.X. Wu, Y. Wang, J.H. Zhu, R. Lai, X.G. Jiang, D.H. Ling, M.C. Prescott, H.H. Rees, Odorranalectin is a small peptide lectin with potential for drug delivery and targeting, PLoS One 3 (2008) e23813.
[23] M.P. Melgarejo, M.D. Hellin, M.C. Melgarejo, Olfactory epithelium of the rat: lectin-mediated histochemical studies, An. Otorrinolaringol. Ibero. Am. 25 (1998) 471–480.
[24] B. Lundh, U. Brockstedt, K. Kristensson, Lectin-binding pattern of neuroepithelial and respiratory epithelial cells in the mouse nasal cavity, Histochem. J. 21 (1989) 33–43.
[25] J.X. Li, X.Q. Xu, C.H. Xu, W.P. Zhou, K.Y. Zhang, H.N. Yu, Y.P. Zhang, Y.T. Zheng, H.H. Rees, R. Lai, D.M. Yang, J. Wu, Anti-infection peptidommics of amphibian skin, Mol. Cell. Proteom. 6 (2007) 882–894.
[26] T. Mamiya, M. Ukai, [Gly14]-Humanin improved the learning and memory impairment induced by scopolamine in vivo, Br. J. Pharmacol. 134 (2001) 1597–1599.

[27] I. Nishimoto, M. Matsuoka, T. Niikura, Unravelling the role of humanin, Trends Mol. Med. 10 (2004) 102–105.
[28] T. Niikura, T. Chiba, S. Aiso, M. Matsuoka, I. Nishimoto, Humanin: after the discovery, Mol. Neurobiol. 30 (2004) 327–340.
[29] H. Tajima, M. Kawasumi, T. Chiba, M. Yamada, K. Yamashita, M. Nawa, Y. Kita, K. Kouyama, S. Aiso, M. Matsuoka, T. Niikura, I. Nishimoto, A humanin derivative, S14G-HN, prevents amyloid – induced memory impairment in mice, J. Neurosci. Res. 79 (2005) 714–723.
[30] M. Yamada, T. Chiba, J. Sasabe, K. Terashita, S. Aiso, M. Matsuoka, Nasal Colivelin treatment ameliorates memory impairment related to Alzheimer's disease, Neuropsychopharmacology 33 (2008) 2020–2032.
[31] T. Niikura, E. Sidahmed, C. Hirata-Fukae, P.S. Aisen, Y. Matsuoka, A humanin derivative reduces amyloid beta accumulation and ameliorates memory deficit in triple transgenic mice, PLoS One 6 (2011) e16259.
[32] P.T. Spicer, K.L. Hayden, Novel process for producing cubic liquid crystalline nanoparticles (cubosmes), Langmuir 17 (2001) 5748–5756.
[33] A. Porjazoska, O.K. Yilmaz, K. Aysal, M. Cvetkovska, S. Sirvanci, F. Ercan, B.M. Baysal, Synthesis and characterization of poly(ethylene glycol)-poly(D,L-lactide-co-glycolide) poly(ethylene glycol) tri-block co-polymers modified with collagen: a model surface suitable for cell interaction, J. Biomater. Sci. Polym. Ed. 17 (2006) 323–340.
[34] R.C. Sun, J.M. Fang, J. Tomkinson, Characterization and esterification of hemicelluloses from rye straw, J. Agric. Food Chem. 48 (2000) 1247–1252.
[35] J. Huwyler, D.F. Wu, W.M. Pardridge, Brain drug delivery of small molecules using immunoliposomes, Proc. Natl. Acad. Sci. USA 93 (1996) 14164–14169.
[36] G.L. Ellman, Tissue sulfhydryl groups, Arch. Biochem. Biophys. 82 (1959) 70–77.
[37] T.G. Van Thienen, J. Demeester, S.C. De Smtdt, Screening poly(ethyleneglycol) micro- and nanogels for drug delivery purposes, Int. J. Pharm. 351 (2008) 174–185.
[38] A.P. Fan, C. Lau, J.Z. Lu, Colloidal gold–polystyrene bead hybrid for chemiluminescent detection of sequence-specific DNA, Analyst 133 (2008) 219–225.
[39] P. Pitzalis, M. Monduzzi, N. Krog, H. Larsson, H. Ljusberg-Wahren, T. Nylander, Characterization of the liquid-crystalline phases in the glycerol monooleate/diglycerol monooleate/water system, Langmuir 16 (2000) 6358–6365.
[40] F.B. Rosevear, The microscopy of the liquid crystalline neat and middle phases of soap and synthetic detergents, J. Am. Oil Chem. Soc. 31 (1954) 628–639.
[41] X.G. Jiang, J.B. Cui, X.L. Fang, Y. Wei, N.Z. Xi, Toxicity of drugs on nasal mucocilia and the method of its evaluation, Acta Pharm. Sin. 30 (1995) 848–853.
[42] J. Davda, V. Labhasetwar, Characterization of nanoparticle uptake by endothelial cells, Int. J. Pharm. 233 (2002) 51–59.
[43] J. Havliš, K. Novotná, J. Havel, Optimization of high performance liquid chromatography separation of neuroprotective peptides fractional experimental designs combined with artificial neural networks, J. Chromatogr. A 1096 (2005) 50–57.
[44] M.I. Lorin, P.F. Gaerlan, I.D. Mandel, Quantitative composition of nasal secretions in normal subjects, J. Lab. Clin. Med. 80 (1972) 275–281.
[45] J. Yuan, Estimation of variance of AUC in animal studies, J. Pharm. Sci. 82 (1993) 761–763.
[46] Q.Z. Zhang, X.G. Jiang, W.M. Jiang, W. Lu, L.N. Su, Z.Q. Shi, Preparation of nimodipine-loaded microemulsion for intranasal delivery and evaluation on the targeting efficiency to the brain, Int. J. Pharm. 275 (2004) 85–96.
[47] C.J. Pike, D. Burdick, A.J. Walencewicz, C.G. Glabe, C.W. Cotman, Neurodegeneration induced by β-amyloid peptides in vitro: the role of peptide assembly state, J. Neurosci. 13 (1993) 1676–1687.
[48] L.K. Simmons, P.C. May, K.J. Tomaselli, R.E. Rydel, K.S. Fuson, E F Brigham, S. Wright, I. Lieberburg, G.W. Becker, D.N. Brems, Secondary structure of amyloid beta peptide correlates with neurotoxic activity in vivo, Mol. Pharmacol. 45 (1994) 373–379.
[49] Y. Peng, C.H. Xing, A. Lemere Cynthia, G.Q. Chen, L. Wang, Y.P. Feng, X.L. Wang, L-3-n-butylphthalide ameliorates beta-amyloid-induced neuronal toxicity in cultured neuronal cells, Neurosci. Lett. 434 (2008) 224–229.
[50] G. Paxinos, C. Watson, The Rat Brain in Stereotaxic Coordinates, sixth ed., Academic Press, New York, 2007.
[51] Y.X. Shen, J. Yang, W. Wei, L.H. Liu, S.Y. Xu, Induction of learning and memory dysfunction by β-amyloid peptide fragment 25–35 in rats, Chin. Pharmacol. Bull. 17 (2001) 26–29.
[52] Y. Yamaguchi, T. Matsuno, S. Kawashima, Antiamnesic effects of azaindolizinone derivative ZSET845 on impaired learning and decreased ChAT activity induced by amyloid-beta 25–35 in the rat, Brain Res. 945 (2002) 259–265.
[53] J. Li, H. Huang, J.M. Miezan Ezoulin, X.L. Gao, F. Massicot, C.Z. Dong, F. Heymans, H.Z. Chen, Pharmacological profile of PMS777, a new AChE inhibitor with PAF antagonistic activity, Int. J. Neuropsychophamacol. 10 (2007) 21–29.
[54] V. Olivier, I. Meisen, B. Meckelein, T.R. Hirst, J. Peter-Katalinic, M.A. Schmidt, A. Frey, Influence of targeting ligand flexibility on receptor binding of particulate drug delivery systems, Bioconjugate Chem. 14 (2003) 1203–1208.
[55] M.P. Xiong, M.L. Forrest, A.L. Karls, G.S. Kwon, Biotin-triggered release of poly(ethylene glycol)-avidin from biotinylated polyethylenimine enhances in vitro gene expression, Bioconjugate Chem. 18 (2007) 746–753.
[56] W.H. Frey II, Bypassing the blood–brain barrier to delivery therapeutic agents to the brain and spinal cord, Drug Deliv. Tech. 2 (2002) 46–49.
[57] R.G. Thorne, G.J. Pronk, V. Padmanabhan, W.H. Frey II, Delivery of insulin-like growth factor-I to the rat brain and spinal cord along olfactory and trigeminal pathways following intranasal administration, Neuroscience 127 (2004) 481–496.
[58] N. Hussain, P.U. Jani, A.T. Florence, Enhanced oral uptake of tomato lectin-conjugated nanoparticles in the rat, Pharm. Res. 14 (1997) 613–618.
[59] T. Chiba, M. Yamada, J. Sasabe, K. Terashita, M. Shimoda, M. Matsuoka, S. Aiso, Amyloid-beta causes memory impairment by disturbing the JAK2/STAT3 axis in hippocampal neurons, Mol. Psychiatry 14 (2009) 206–222.
[60] L. Illum, Transport of drugs from the nasal cavity to the central nervous system, Eur. J. Pharm. Sci. 11 (2000) 1–18.